Antisolvent Precipitation for Metal Recovery from Citric Acid Solution in Recycling of NMC Cathode Materials

Wen Xuan, Alexandre Chagnes, Xiong Xiao, Richard Olsson, Kerstin Forsberg

metals

MDPI

Article

Antisolvent Precipitation for Metal Recovery from Citric Acid Solution in Recycling of NMC Cathode Materials

Wen Xuan [1], Alexandre Chagnes [1,*], Xiong Xiao [2], Richard T. Olsson [2] and Kerstin Forsberg [3,*]

[1] GeoRessources, Université de Lorraine, CNRS, F-54000 Nancy, France; wen.xuan@univ-lorraine.fr
[2] Department of Fibre and Polymer Technology, KTH Royal Institute of Technology, 10044 Stockholm, Sweden; xiongxi@kth.se (X.X.); rols@kth.se (R.T.O.)
[3] Department of Chemical Engineering, KTH Royal Institute of Technology, 10044 Stockholm, Sweden
* Correspondence: alexandre.chagnes@univ-lorraine.fr (A.C.); kerstino@kth.se (K.F.)

Abstract: Lithium-ion batteries (LIBs) are widely used everywhere today, and their recycling is very important. This paper addresses the recovery of metals from NMC111 ($LiNi_{1/3}Mn_{1/3}Co_{1/3}O_2$) cathodic materials by leaching followed by antisolvent precipitation. Ultrasound-assisted leaching of the cathodic material was performed in 1.5 mol L^{-1} citric acid at 50 °C and at a solid-to-liquid ratio of 20 g/L. Nickel(II), manganese(II) and cobalt(II) were precipitated from the leach liquor as citrates at 25 °C by adding an antisolvent (acetone or ethanol). No lithium(I) precipitation occurred under the experimental conditions, allowing for lithium separation. The precipitation efficiencies of manganese(II), cobalt(II) and nickel(II) decreased according to the order Mn > Co > Ni. The precipitation efficiency increased when a greater volume of antisolvent to the leachate was used. A smaller volume of acetone than ethanol was needed to reach the same precipitation efficiency in accordance with the difference in the dielectric constants of ethanol and acetone and their associated solubility constants. After adding two volumes of acetone into one volume of the leach liquor, 99.7% manganese, 97.0% cobalt and 86.9% nickel were recovered after 120 h, leaving lithium in the liquid phase. The metal citrates were converted into metal oxides by calcination at 900 °C.

Keywords: lithium-ion batteries; NMC111; cathode; recycling; hydrometallurgy; antisolvent; precipitation; leaching; citric acid

Citation: Xuan, W.; Chagnes, A.; Xiao, X.; Olsson, R.T.; Forsberg, K. Antisolvent Precipitation for Metal Recovery from Citric Acid Solution in Recycling of NMC Cathode Materials. *Metals* **2022**, *12*, 607. https://doi.org/10.3390/met12040607

Academic Editor: Jiro Kitagawa

Received: 4 March 2022
Accepted: 30 March 2022
Published: 31 March 2022

1. Introduction

The lithium-ion battery (LIB) is a widely used energy storage technology for electric vehicles. The energy storage capacity has multiplied more than 8.5 times in 10 years only. In 2009, there were nearly 25.6 GWh (134,000 tons) of LIB energy storage capacity placed on the global market. In 2019, this was about 218 GWh (over 1.2 million tons), and it is expected that more than 2500 GWh (over 12.7 million tons) will be on the market in 2030, which will subsequently result in a vast amount of waste from both LIB production and spent LIBs [1]. In the production of LIBs, different waste streams enriched with electrode materials are generated. It is necessary to develop new processes to recycle the valuable elements from battery waste [2,3]. A common LIB cathode material in use today is $LiNi_{1/3}Mn_{1/3}Co_{1/3}O_2$, also called NMC111 [4]. In the future, it is foreseen that NMC111 will be replaced by Ni-rich cathode materials like NMC811. It is important to develop adequate processes to recover Li, Ni, Mn and Co from these types of waste electrodes.

In the last decade, many hydrometallurgical and pyrometallurgical processes have been developed to recover valuable metals from spent LIBs. These processes rely on different types of chemistry and the implementation of several operations to recover and separate the metals including shredding, crushing/grinding, physical concentration, calcination, leaching, liquid–liquid and solid–liquid extraction, as well as precipitation [5]. Pyrometallurgical recycling processes have high investment costs and are best suited for

batteries with high contents of nickel and cobalt [6]. Current pyrometallurgical approaches need further refinement, e.g., by combining with hydrometallurgical processing to recover all metals; especially, the recovery of lithium must be enhanced [6]. Hydrometallurgical battery recycling processes offer the opportunity to achieve high recovery rates, necessary to comply with future legislation, and the possibility to produce new battery precursors [6].

Precipitation is used in hydrometallurgy for the separation, purification or production of salts and also for removing impurities [7]. In the field of precipitation and crystallization, evaporative crystallization is a mature technique for producing salts. However, evaporative crystallization is an energy-intensive process. Since large amounts of heat must be exchanged, the capital investment is also very high because of the oversized heat transfer surface area. Substantial savings can be made, provided that the salt-water separation can be done without vaporizing water [8]. In addition to high costs, evaporative crystallization does not allow controlling supersaturation in an appropriate way. Consequently, the fine crystal particles may agglomerate with impurities and the solid purity may drastically decrease [7]. Antisolvent precipitation or organic displacement crystallization is an energy-saving alternative that offers interesting possibilities to better control the crystallization process [9]; this technique is based on changing the solubility of the solute and creating a supersaturated solution by adding a water-miscible organic solvent to force the solute to precipitate [10]. This technique is widely used in the pharmaceutical industry [11–15].

A hydrometallurgical process usually involves a first step of dissolution to recover all the metals in an aqueous phase before several steps to separate and to purify each one of them [16]. Sulfuric acid and hydrochloric acid are mostly used for cathode digestion [17–19]. Antisolvent precipitation of rare-earth elements, nickel and cobalt from sulfuric acid leachate of NiMH electrodes, has been reported [10,20]. In a chloride system, it is difficult to precipitate metals due to formation of chloro-complexes with high solubility [7]. Organic acids may be environmentally sustainable alternatives for the cathode dissolution [21]. Citric acid has been reported to be a green and efficient reagent to dissolve metals from spent lithium nickel manganese cobalt oxides (NMC) electrodes and blackmass [22,23]. The use of citric acid does not produce toxic emissions and it is a cost-efficient solvent [24,25]. Citric acid is a weak acid but has a strong chelating ability, which provides it with good leaching capability. However, the chelating property can also introduce challenges in efficient separation and recovery of elements [24]. Solvent extraction can be applied after leaching of LIB electrode material by citric acid to separate and recover the main elements (Ni, Mn, Co, Al and Li) [24]. The extractant D2EHPA diluted in kerosene can extract Mn, Al at a pH of 2.5 and Li at a pH of 5.5. Citric acid can then be used to efficiently strip Mn and Li from the respective loaded organic phases. There is still a need for further research to develop efficient closed-loop citric-acid-based recycling processes, especially the downstream purification and separation steps [24,25].

In this study, antisolvent precipitation was assayed to precipitate nickel(II), cobalt(II) and manganese(II) from citric acid. To the best of our knowledge, antisolvent precipitation has not been applied after organic acid leaching of NMC materials. The resulting precipitates were afterwards calcined to produce new metal oxides.

2. Materials and Methods

2.1. Materials

The lithium nickel-manganese-cobalt oxide (NMC111, purity > 98%) was purchased from Sigma-Aldrich (Burlington, MA, USA). Manganese carbonate ($MnCO_3$, purity = 99.9%), nickel hydroxide ($Ni(OH)_2$, Ni 61%) and lithium hydroxide anhydrous (LiOH, purity = 98%) were purchased from Alfa Aesar (Ward Hill, MA, USA). Cobalt carbonate hydrate ($CoCO_3 \cdot xH_2O$, Co 45.5%) was purchased from Acros Organics (Geel, Antwerp, Belgium). Nitric acid (HNO_3, 69%) was purchased from VWR (Radnor, PA, USA). Citric acid ($C_6H_8O_7$, purity $\geq$ 99.5%), acetone (CH_3COCH_3, purity > 99.5%) and anhydrous ethanol (CH_3CH_2OH, purity $\geq$ 99.5%) were purchased from Sigma-Aldrich. Monoelement standard solutions containing 1000 mg L^{-1} Li, Ni, Co, or Mn in 2–5 w% HNO_3 or HCl (Alfa Aesar) were

used for inductively coupled plasma-optical emission spectrometry (ICP-OES) calibration. All chemical reagents were used as received without further purification. MiliQ water (>18.2 MΩ·cm) was used in all the experiments.

The agitation was performed by a 2mag MIXdrive 60 (2magAG, Munich, Germanry) with a MIXcontrol 40 controller unit operated at 400 rpm immersed in a thermostatic water bath (Lauda LCB 4743 Model E 20 G). A KDS 100 Legacy syringe pump (KD Scientific Inc., Holliston, MA, USA) was used to control the injection rate of antisolvent into the aqueous phase.

The liquid samples were taken using a syringe and filtering off the solid through a Whatman 6900-2502 GD/X 25 Sterile Syringe Filter (Whatman plc, Buckinghamshire, UK) (pore size = 0.2 µm).

2.2. Leaching of NMC111

Carboxylic acids, and more especially citric acid, have been reported in the literature as environmentally friendly reagents, which may be relevant for leaching cathodic materials from spent LIBs despite their weak acidity. In particular, the complexing properties of citrate regarding transition metals is an asset for leaching operations [26]. The leaching of NMC111 by a monoprotonic acid (quoted HOA) occurs according to the following reaction [27]:

$$6LiNi_{1/3}Mn_{1/3}Co_{1/3}O_2(s) + 18HOA(aq) + 3H_2O_2(l) = 2Ni(OA)_2(aq) + 2Mn(OA)_2(aq) + 2Co(OA)_2(aq) + 6LiOA(aq) + 3O_2(g) + 12H_2O(l) \quad (1)$$

There is no information in the literature about the leaching reaction of NMC111 by citric acid, but it can be expected that the mechanisms may be close to the reaction reported in Equation (1). Considering the overall leaching reaction, poor leaching efficiencies of $LiCoO_2$ are obtained without the addition of a suitable reductant to reduce cobalt(III) and manganese(VI) to cobalt(II) and manganese(II), respectively [28]. However, the leaching kinetics can be improved in the absence of hydrogen peroxide by using ultrasound waves to take advantage of cavitation formation. When the pressure in the cavitation increases, a large amount of energy is released. This energy is responsible for micro-crack formation on the cathodic material surface that accelerates the leaching agent diffusion into the cathodic material [29]. Thus, ultrasonic agitation was experimentally proved to be more efficient than mechanical stirring [30]. Therefore, ultrasonic agitation was implemented during leaching in the present work. The optimized leaching conditions were taken from the work of Xiao et al. [23].

The leaching experiments were performed in 500 mL three-necked round-bottom flasks equipped with condenser units to recirculate any evaporated liquid. Typically, the round-bottom flask was placed in the same position in an ultrasonic bath (BRANSON 2800 CPX2800H-E, Emerson, St. Louis, MO, USA, with a max sonics power of 110 W at a frequency of 40 kHz). The ultrasound bath temperature was maintained at 50 °C (±2 °C). After 24 h of ultrasonic-assisted leaching, the leachate was collected by centrifugation at 4000 rpm to remove any solid phase. Leaching experiments were carried out using 1.5 mol L^{-1} citric acid at a solid-to-liquid ratio S/L = 40 g L^{-1} (Exp. 1, Table 1) and 20 g L^{-1} (Exp. 2, Table 1).

Table 1. Leach liquor composition after NMC dissolution assisted by ultrasound in 1.5 mol L^{-1} citric acid at 50 °C.

Exp.	S/L (g/L)	pH	Leachate Composition Molality (mmol Kg^{-1})				Leaching Efficiency (%)			
			Li	Ni	Mn	Co	Li	Ni	Mn	Co
1 *	40	2.91	404	99	24	62	87	63	15	39
2	20	2.53	189	57	73	63	82	74	95	81

* Precipitation occurred during leaching.

The composition of the leach liquors from experiments 1 and 2 are presented in Table 1. In Exp. 1 (S/L = 40 g L^{-1}, Table 1), precipitation occurred during leaching. After filtration and drying, X-Ray powder Diffraction (XRD) showed the presence of $Mn(HC_6H_5O_7)\cdot H_2O$ in the solid (Supplementary Materials, Figure S1) [31]. No precipitation was visually observed in Exp. 2 (S/L = 20 g L^{-1}, Table 1). The liquor from Exp. 2 was used for antisolvent precipitation experiments. The pH of this solution was 2.0.

2.3. Antisolvent Precipitation from Single Metal Systems

Separate solutions of lithium(I), nickel(II), manganese(II) and cobalt(II) were prepared by dissolving the corresponding salts in 1.5 mol L^{-1} citric acid according to the experimental conditions reported in Table 2. The final concentrations of the elements were chosen to be in the same range as after NMC leaching using 1.5 mol L^{-1} citric acid and a solid-to-liquid ratio of 20 (see Table 1).

Table 2. Salt dissolution in 1.5 mol L^{-1} citric acid.

Metal Ion	Salt	Temperature (°C)	Agitation Time (h)	Final Metal Concentration (mg L^{-1})
Lithium(I)	LiOH	25	8	1455
Nickel(II)	$Ni(OH)_2$	60	10	3648
Manganese(II)	$MnCO_3$	25	1	3786
Cobalt(II)	$CoCO_3$	60	10	3873

The precipitation experiments were carried out in high-density polyethylene (HDPE) bottles equipped with polytetrafluoroethylene (PTFE)-coated stirrer bars and agitated using submersible magnetic stirrers inside a water bath set at a temperature of 25 °C, equipped with a temperature sensor (accuracy = ±0.01 °C). The stirring rate was kept constant in all the experiments at 400 rpm to keep all material suspended. The HDPE bottles were sealed to prevent solvent evaporation. The initial volume of the aqueous phase was 10 mL. Acetone or ethanol were added all at once (one-pot addition) using a burette or at a rate of 0.5 mL min^{-1} using a syringe pump (KD Scientific 200P infusion, KD Scientific Inc., Holliston, MA, USA) to reach the targeted initial antisolvent-to-aqueous volumetric ratios (O/A). After adding the antisolvent, the solutions were left under stirring. The experimental conditions implemented for the antisolvent precipitation are summarized in Table 3.

During stirring, samples of clear solution were collected regularly using a syringe equipped with a Whatman 6900-2502 GD/X 25 Sterile Syringe Filter (Whatman plc, Buckinghamshire, UK) (pore size = 0.2 µm). The liquid samples were immediately diluted 100 times with 5 v/v% HNO_3 solution and stored in HDPE bottles before ICP-OES analyses. The volume and weight of each sample and antisolvent added in the sample were recorded.

The solids were filtered off using a vacuum pump system that contained a Büchner funnel and Muntktell qualitative filter paper Grade 3 (Ahlstrom-Munksjö, Helsinki, Finland). The solid samples were washed with the same citric acid-antisolvent mixture that was used for the antisolvent precipitation. Afterwards, the solids were dried at room temperature in a fume hood for 24 h before performing powder X-ray diffraction analyses.

2.4. Antisolvent Precipitation from NMC111 Leach Liquor

The same general procedure as for the single metal systems was used to investigate the antisolvent precipitation from the NMC111 leach liquor. The liquor was prepared according to Exp. 2 reported in Table 1. The total volume of initial leach liquor in each experiment was 10 mL. The stirring rate was kept constant in all the experiments at 400 rpm and the temperature was 25 °C. The experimental conditions are given in Table 4.

Table 3. Experimental conditions for the antisolvent precipitation experiments from single metal systems (Table 2). The temperature was kept constant at 25 °C.

Exp.	Metal Ion	Initial Total Metal Concentration (mmol Kg^{-1})	Antisolvent	Antisolvent Addition Rate (mL min^{-1})	Final Antisolvent-to-Aqueous (O/A) Volumetric Ratio	Time of Experiment (h)
L1	Li	189.5	Acetone	One-pot	0.25	336
L2	Li	189.5	Acetone	One-pot	0.5	336
L3	Li	189.5	Acetone	One-pot	1	336
L4	Li	189.5	Ethanol	One-pot	0.25	336
L5	Li	189.5	Ethanol	One-pot	0.5	336
L6	Li	189.5	Ethanol	One-pot	1	336
L7	Li	189.5	Ethanol	One-pot	2	336
N1	Ni	56.3	Acetone	One-pot	0.25	380
N2	Ni	56.3	Acetone	One-pot	0.5	380
N3	Ni	56.3	Acetone	One-pot	1	380
N4	Ni	56.3	Ethanol	One-pot	0.25	380
N5	Ni	56.3	Ethanol	One-pot	0.5	380
N6	Ni	56.3	Ethanol	One-pot	1	380
N7	Ni	56.3	Ethanol	One-pot	2	380
N8	Ni	182.9	Acetone	0.5	2	250
M1	Mn	62.5	Acetone	One-pot	0.25	380
M2	Mn	62.5	Acetone	One-pot	0.5	380
M3	Mn	62.5	Acetone	One-pot	1	380
M4	Mn	62.5	Ethanol	One-pot	0.25	380
M5	Mn	62.5	Ethanol	One-pot	0.5	380
M6	Mn	62.5	Ethanol	One-pot	1	380
M7	Mn	62.5	Ethanol	One-pot	2	380
C1	Co	59.6	Acetone	One-pot	0.25	380
C2	Co	59.6	Acetone	One-pot	0.5	380
C3	Co	59.6	Acetone	One-pot	1	380
C4	Co	59.6	Ethanol	One-pot	0.25	380
C5	Co	59.6	Ethanol	One-pot	0.5	380
C6	Co	59.6	Ethanol	One-pot	1	380
C7	Co	59.6	Ethanol	One-pot	2	380
C8	Co	59.6	Acetone	0.5	2	321

Table 4. Experimental conditions for the antisolvent precipitation from NMC leach liquor from experiment 2 (Table 1). The temperature was kept constant at 25 °C.

Exp.	Antisolvent	Antisolvent Addition Rate (mL/min)	Final Antisolvent-to-Aqueous Volumetric Ratio (O/A)	Experiment Duration (h)
LNMC1	Acetone	One-pot	0.25	758
LNMC2	Acetone	One-pot	0.5	506
LNMC3	Acetone	One-pot	1	505
LNMC4	Acetone	One-pot	2	516
LNMC5	Ethanol	One-pot	0.25	758
LNMC6	Ethanol	One-pot	0.5	506
LNMC7	Ethanol	One-pot	1	505
LNMC8	Ethanol	One-pot	2	516
LNMC9	Acetone	0.5	1	24
LNMC10	Acetone	0.5	2	24

2.5. Analysis

Prior to ICP-OES analyses with the Thermo Scientific iCAP 7000 Series (Thermofisher Scientific, Waltham, MA, USA), the samples were diluted in 5% (vol.) nitric acid. Lithium, nickel, manganese and cobalt concentrations in aqueous solutions were determined by ICP-OES at 460.286 nm and 610.362 nm for lithium; 221.647 nm, 300.249 nm and 352.454 nm for nickel; 257.610 nm, 259.373 nm and 403.076 nm for manganese; and 228.616 nm, 231.160 nm

and 237.862 nm for cobalt. The precision was good with a relative standard deviation of <1%. Monoelemental standards containing 1000 mg L^{-1} cobalt, nickel, manganese and lithium in 2–5% (vol.) HNO_3 were used for calibration.

Metal concentrations determined by ICP-OES after precipitation experiments were used to calculate the precipitation efficiencies defined as follows by assuming that the volume change in the liquid phase during precipitation was negligible:

$$\%PE(M) = \frac{[M]_i m_i - [M]_f m_f}{[M]_i m_i} \times 100\% \quad (2)$$

where $[M]_i$ is the concentration of the metal (M) in the initial solution in mol kg^{-1}; m_i is the solvent (citric acid) weight in the initial solution in kg; $[M]_f$ is the final concentration of the metal (M) in the organic-aqueous mixture expressed in molality (mol kg^{-1}) after filtering off the precipitate; and m_f is the solvent weight in the final solution (citric acid and antisolvent).

The precipitates were characterized by X-ray diffraction (XRD) and thermogravimetric analysis (TGA). The TGA analyses were performed by using a Netzsch STA 449 F3 Jupiter (Netzsch Gruppe, Selb, Germany) between 25 °C and 1000 °C at a ramp speed of 15 °C min^{-1} under an air atmosphere. X-ray diffraction of the precipitates before and after calcination was performed with a PANalytical X'Pert Pro (Malvern Instruments, Malvern, UK). The X-ray diffraction patterns were recorded over a 2θ range from 5° to 90° with steps of 0.02° at 45 kV and 40 mA using Cu Kα radiation (λ = 0.15418 nm). Attenuated total reflectance Fourier transform infrared spectroscopy (ATR-FTIR; Perkin Elmer Spectrum Two, PerkinElmer, Waltham (HQ), MA, USA) was used to measure the IR spectra of the precipitate obtained after adding acetone at O/A = 2 (LNMC4). The same precipitate was also dissolved, and the metal composition was determined by ICP-OES analysis.

Calcination experiments were performed in a Mettler-Toledo furnace (TGA/SDTA851, Mettler Toledo, Greifensee, Switzerland) from 30 °C to 900 °C at 10°C min^{-1} under 50 mL min^{-1} oxygen flow. The samples were maintained at 900 °C for 1 h inside the furnace before natural cooling down to room temperature.

3. Results and Discussion

3.1. Antisolvent Precipitation from Synthetic Solutions (Single Metal Systems)

Precipitation of lithium(I), manganese(II), cobalt(II) and nickel(II) from citric acid was investigated at 25 °C by adding ethanol or acetone as antisolvent. A good selectivity towards manganese(II), cobalt(II) and nickel(II) was observed as no lithium(I) precipitation occurred after adding acetone or ethanol even after 14 days.

The addition of acetone or ethanol into citric acid containing initially 63 mmol kg^{-1} manganese(II) was responsible for manganese(II) precipitation except with ethanol at O/A = 0.25 (Figure 1a). In the presence of ethanol, it is indeed mandatory to increase the O/A values to observe manganese(II) precipitation. At O/A = 0.5, manganese(II) precipitation occurred but the precipitation rate was lower than in the presence of acetone. The kinetics of precipitation were almost the same in the presence of ethanol or acetone at O/A = 1. It can be inferred that high values of O/A promote the nucleation processes. At O/A = 2, 93% of manganese(II) precipitated when ethanol was used as antisolvent. The use of acetone seems to be more suitable for antisolvent precipitation since a smaller amount of acetone is necessary to precipitate manganese(II) efficiently.

Nickel(II) and cobalt(II) precipitation from citric acid were investigated under the same conditions as for manganese(II). Precipitation experiments were performed only at O/A = 1 with acetone and O/A = 2 with ethanol according to the preceding results showing that high values of O/A led to efficient and fast precipitation of manganese(II). Nickel(II) and cobalt(II) behaviors were quite different as no nickel(II) precipitation occurred even after 14 days in the presence of acetone (Exp. N7 in Table 3), whereas cobalt(II) started precipitating after 10 days under the same experimental conditions (Figure 1b). Such an observation is particularly surprising as nickel(II) and cobalt(II) are normally difficult to separate and usually precipitate together between pH 8.2 and 8.8 in the presence of a

neutralizing agent such as MgO pulp [32]. Figure 1c shows that 24% nickel(II) precipitation was eventually observed after 10 days in the presence of acetone provided that initial nickel(II) concentration was higher (190 mmol kg^{-1} instead of 62.6 mmol kg^{-1}) and acetone was added to a phase volume ratio O/A = 2 (Exp. N8 in Table 3).

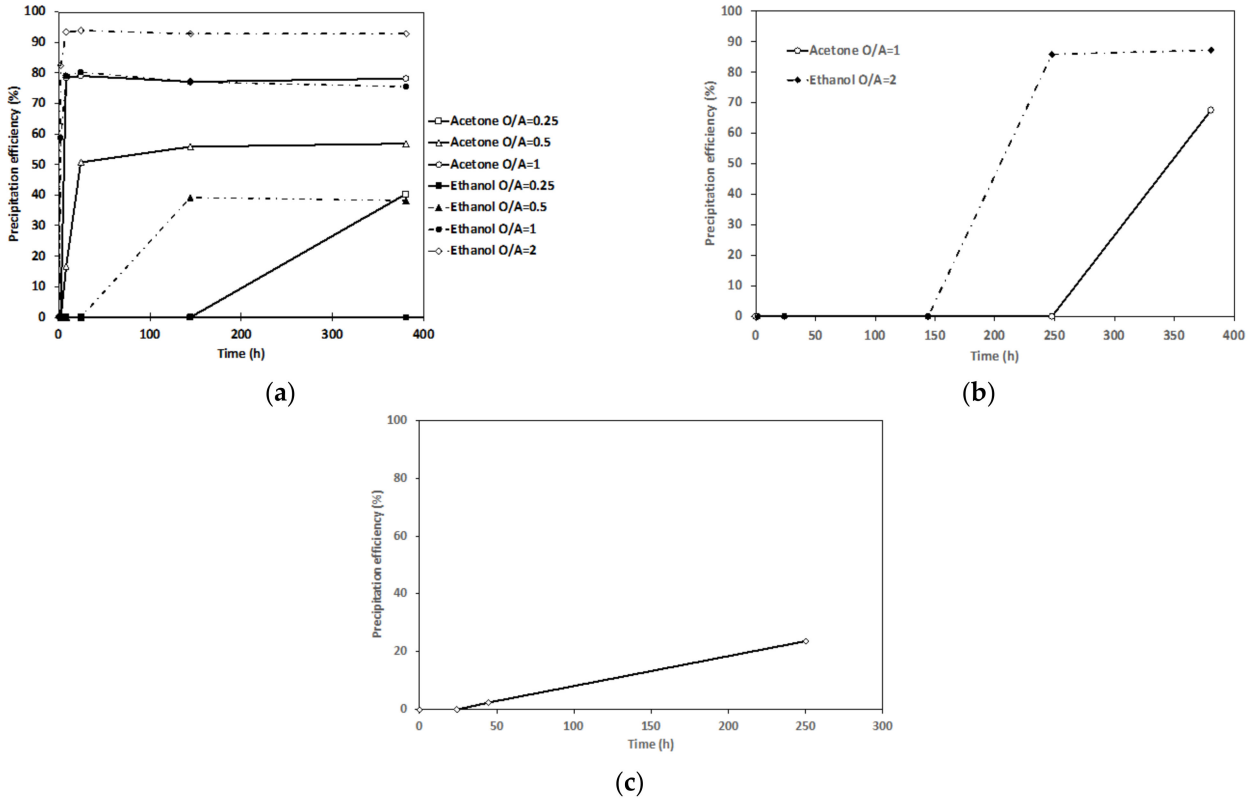

Figure 1. Precipitation efficiency at 25 °C of (**a**) manganese(II) (Exp. M1–M7 in Table 2), (**b**) cobalt(II) (Exp. C3 and C7 in Table 2) and (**c**) nickel(II) (Exp. N8 in Table 3) from single metal solutions.

Regarding the cobalt(II) precipitation, significant precipitation was only observed after 10 days and 16 days after the addition of acetone at O/A = 1 and ethanol at O/A = 2, respectively. The comparison of Figures 1a and 1b shows that the system needs a longer time to nucleate (the induction time is longer) for cobalt(II) than for manganese(II). Due to the unknown speciation in the mixed-solvent systems, it is not possible to compare the results at the same supersaturation driving force.

As a conclusion, the addition of a solvent for which the dielectric constant is lower than water (e_r(water) = 79.99, e_r(ethanol) = 25.02 and e_r(acetone) = 21.30 at 25 °C according to [33]) into the citric acid aqueous solutions promotes the nickel(II) and manganese(II) precipitation, whereas nickel(II) remains difficult to precipitate. Coulomb's law shows that the force of interaction between the charges is inversely proportional to the dielectric constant. Therefore, it can be assumed that the solubility of salts relates to the dielectric constant of the medium. Thus, the addition of ethanol or acetone (e_r(ethanol) = 25.02 and e_r(acetone) = 21.30) into an aqueous solution (e_r = 80) creates supersaturation allowing strong variation of the crystallization process conditions [34].

All precipitates before and after calcination were characterized by XRD. The XRD pattern of the Mn(II) precipitate obtained in Exp. M7 (Table 3) shows the presence of $Mn(HC_6H_5O_7)\cdot H_2O$ [35] and other phases, which were not identified (Supplementary Materials, Figure S2). Likewise, the Co(II) precipitate obtained in Exp. C7 could not be identified (Supplementary Materials, Figure S3). Citric acid is commonly used in gel combustion synthesis of metal oxides and the tendency for formation of amorphous metal citrate precursors or gels in these systems is well-known [35–37]. Nevertheless, the crystal quality can potentially be improved by controlling the antisolvent addition rate in order to

maintain a lower degree of supersaturation during nucleation and crystal growth [38]. In experiment N8 (Ni) the antisolvent was added to the leach solution at a rate of 0.5 mL/min. However, analysis of the XRD pattern of the nickel(II) salt obtained in Exp. N8 did not permit identification of the solid phase(s) (Figure S4 in the Supplementary Materials). After calcination of manganese(II), cobalt(II) and nickel(II) precipitates, the XRD patterns showed the presence of Mn_2O_3 (JCPDS card no. 24-0508), Co_3O_4 (JCPDS card no. 42-1467) and NiO (JCPDS card no. 47-1049), respectively (Figure 2).

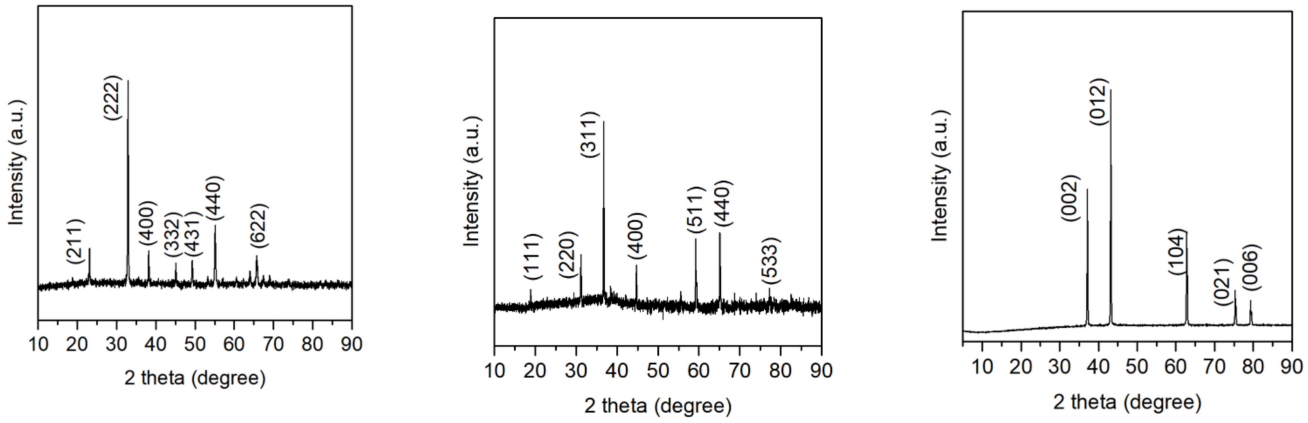

Figure 2. XRD patterns after calcination of the solid obtained by anti-solvent precipitation of (**a**) manganese(II) (Exp. M7), (**b**) cobalt(II) (Exp. C7) and (**c**) nickel(II) (Exp. N7).

3.2. Antisolvent Precipitation from NMC111 Leach Solution (Mixed Metal Systems)

After the addition of ethanol or acetone into the leach solution at 25 °C and at O/A = 0.25, 0.5, 1 and 2, manganese(II), cobalt(II) and nickel(II) precipitated while lithium remained in the solution. The precipitation efficiencies of Ni, Mn and Co are presented in Figures 3 and 4. The precipitate obtained after adding acetone at O/A = 2 (LNMC4) contained 4.2% Ni, 7.5% Mn, 6.8% Co and 0.09% Li by mass. The time until nucleation occurred decreased as the O/A ratio increased, e.g., no precipitation was observed until after 100 h after adding ethanol at O/A = 0.25 while precipitation was observed immediately after addition of the antisolvent at O/A = 2. It can also be seen that the concentration of manganese(II), cobalt(II) and nickel(II) in solution decreased more rapidly at the highest O/A ratios and the final precipitation efficiencies were higher. This is in accordance with the higher supersaturation driving force for nucleation and crystal growth as more antisolvent was added. The precipitation efficiency decreased in the order Mn > Co > Ni in accordance with the results from the single systems. However, the induction time for cobalt(II) and nickel(II) was much shorter in the mixed systems. This is likely due to the presence of manganese(II), which when precipitating leads to secondary nucleation of the respective nickel and cobalt phases, i.e., the presence of manganese nuclei facilitates cobalt and nickel precipitation.

At the same O/A ratio, the precipitation efficiencies of manganese(II), cobalt(II) and nickel(II) are lower in the presence of ethanol than in the presence of acetone; see Figures 3 and 4. Such an observation is in accordance with the dielectric constants of acetone and ethanol as discussed for the single systems.

The highest precipitation efficiency for all the metals was obtained at O/A = 2 for acetone; see Figure 4. Under these conditions, 99.7% (wt) manganese, 97.0% (wt) cobalt and 86.9% (wt) nickel were recovered as a mixed solid phase.

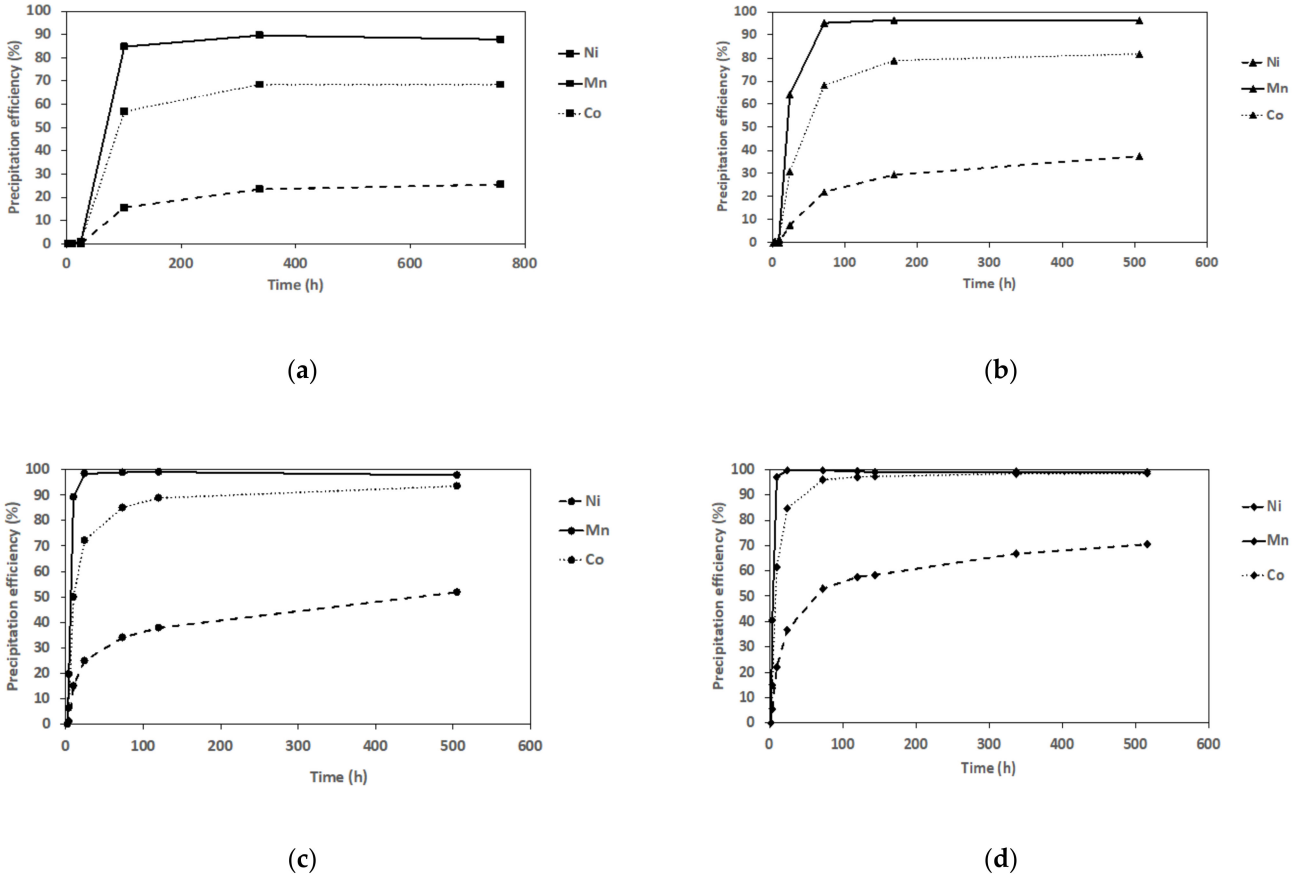

Figure 3. Precipitation efficiency after adding ethanol into the leachate at antisolvent-to-aqueous volumetric ratios (**a**) O/A = 0.25, (**b**) O/A = 0.5, (**c**) O/A = 1 and (**d**) O/A = 2.

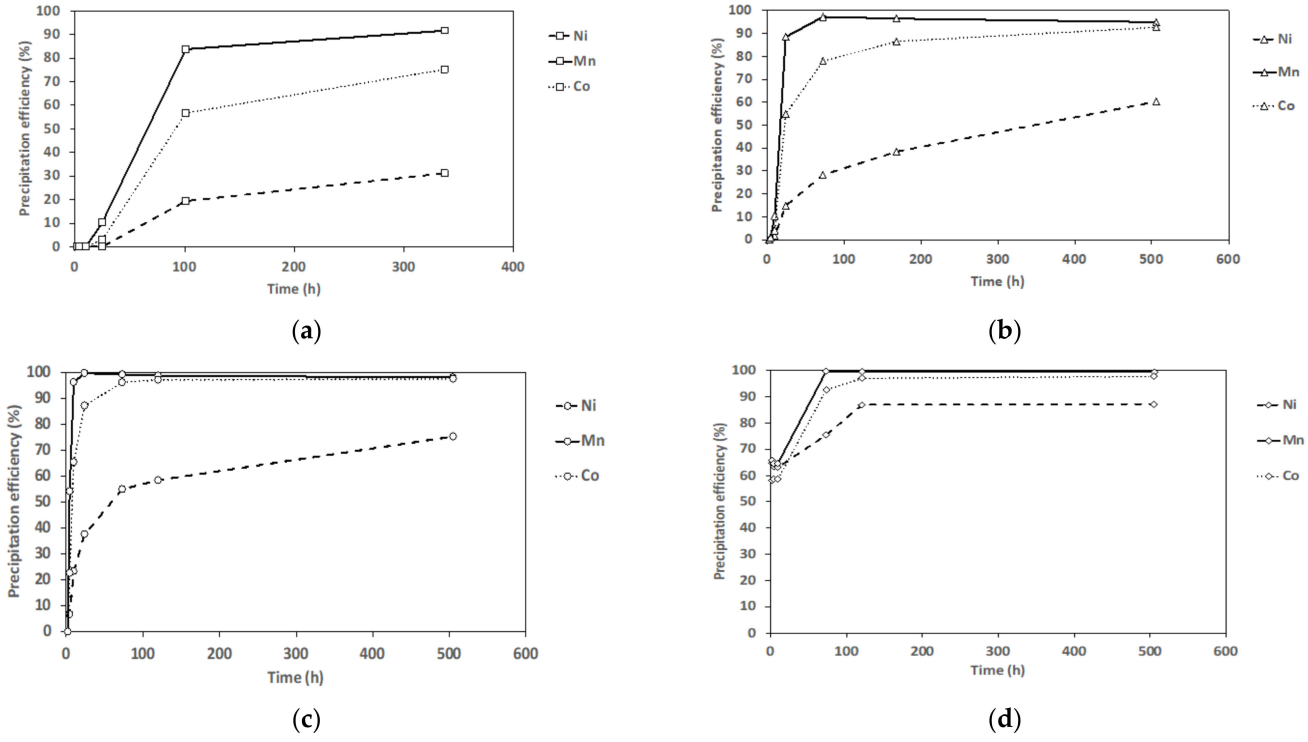

Figure 4. Precipitation efficiency after adding acetone into the leachate at antisolvent-to-aqueous volumetric ratios (**a**) O/A = 0.25, (**b**) O/A = 0.5, (**c**) O/A = 1 and (**d**) O/A = 2.

The precipitations of each element using different antisolvent and O/A are shown in Figure 5. For each element, higher O/A increased the precipitation efficiency. Acetone had a stronger effect to precipitate the metals than ethanol.

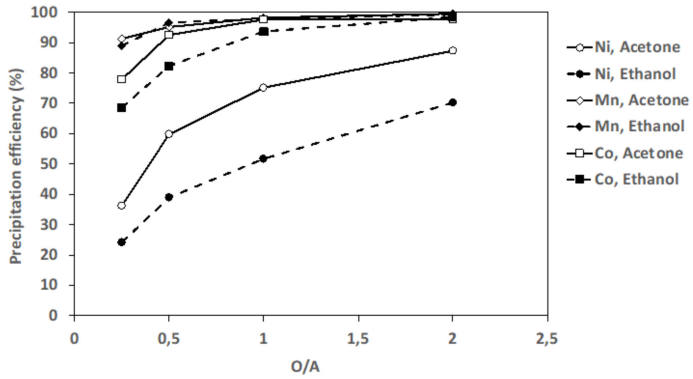

Figure 5. Precipitation efficiency 500 h after adding acetone (solid lines) and ethanol (dashed lines) into leachates at different antisolvent-to-aqueous volumetric ratios (O/A).

The mixed solid phase (Exp. LNMC4) was analyzed by powder-XRD, but the pattern could not be identified; see Figure S5 of the Supplementary Materials. The Fourier transform infrared spectroscopy (FT-IR) spectrum of the precipitate is presented in Figure 6. The spectral peaks close to 3600 cm^{-1} and the neighboring broad bands in the lower region can be attributed to stretching vibrations of water molecules [37], indicating the presence of water. The strong and sharp peaks observed in the regions of 1625–1575 cm^{-1} and 1485–1375 cm^{-1} can be attributed to the characteristic asymmetric and symmetric stretching of carboxylate groups [39], indicating that the solid precipitate is a carboxylate salt.

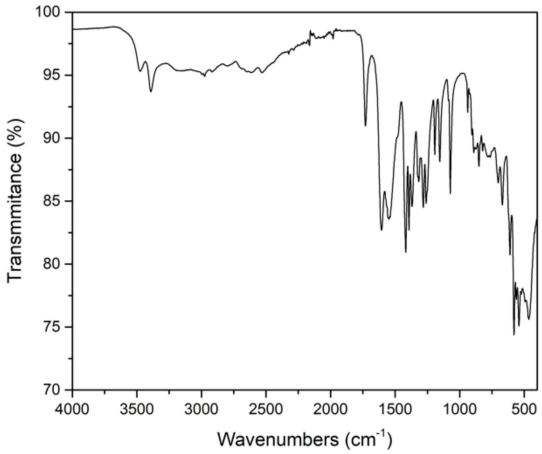

Figure 6. FT-IR spectra of the mixed precipitate (Exp. LNMC4).

Even if the precipitate could not be fully identified, the results indicate that it could be composed of a mixture of metal citrate hydrates or solvates of manganese, cobalt and nickel. The thermogravimetric analysis of the mixed solid phase is reported in Figure 7. Two transition temperatures can be seen: one transition from about 220 °C to 300 °C, which can be attributed to the loss of water; the second transition from about 350 °C to 380 °C may result from the transformation of citrate salt into oxides [35]. The loss of ignition at 1000 °C was 72.5%. The composition of the precipitate obtained after antisolvent crystallization comprised 18.5 mass% of Ni, Mn and Co, which corresponds to 25.8% by mass of metal oxides assuming the presence of only Mn_2O_3, Co_3O_4 and NiO. These results are in fairly good agreement.

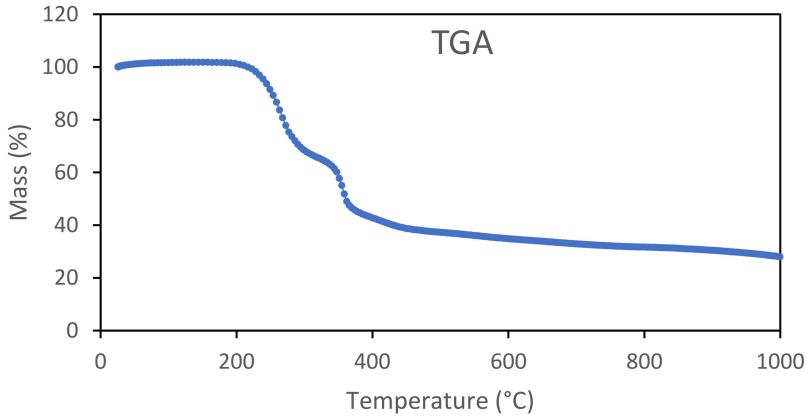

Figure 7. Thermogravimetric analysis (TGA) of the mixed precipitate (Exp. LNMC4).

After calcination at 900 °C the precipitate was transformed into metal oxides; see Figure 8**.** The XRD-pattern matches with $NiMn_2O_4$ or Co_2MnO_4. However, other oxides with similar crystallographic structure could also potentially be considered [40].

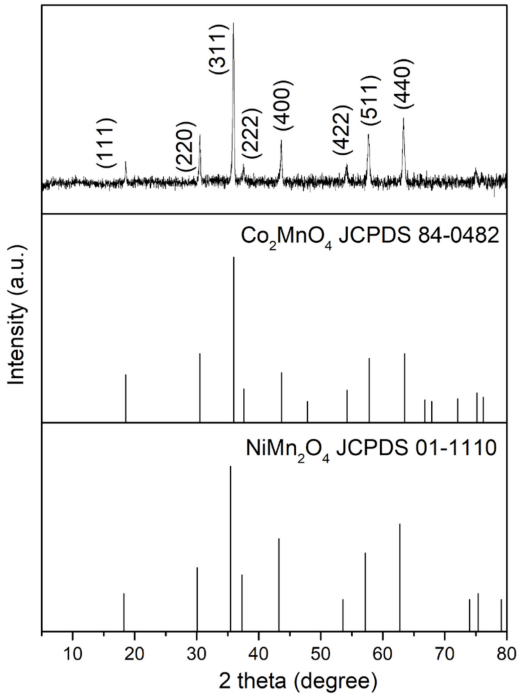

Figure 8. XRD pattern of the mixed precipitate (Exp. LNMC4) after calcination and the reference patterns of Co_2MnO_4 and $NiMn_2O_4$.

To conclude, antisolvent crystallization is an efficient method to precipitate manganese, cobalt and nickel from citric acid solution. In a future process, the antisolvent can be distilled from the remaining citric acid and both liquids can be recirculated to the process. Furthermore, the precipitate can be calcined to obtain a mixed metal oxide product. This is of particular interest since it also opens the possibility for using the precipitate as a precursor for direct synthesis of new NMC cathode material.

The same approach can probably be applicable to separate metals as metal carboxylate salts from a wide variety of carboxylic acid solutions of relevance for many processes where these green solvents are used for leaching or stripping of metal ions.

4. Conclusions

Manganese(II), cobalt(II) and nickel(II) can be precipitated from citric acid solution by adding acetone or ethanol as the antisolvent. The precipitation efficiency increases as the amount of antisolvent added increases. A lower amount of acetone than ethanol is needed to reach the same precipitation efficiency under comparable conditions. The precipitation efficiency follows the order Mn > Co > Ni. After adding two volumes of acetone into one volume of the leach liquor, 99% Mn, 98% Co and 87% Ni by weight were recovered after 120 h, leaving lithium in the liquid phase. This process paves the way to separate manganese, cobalt and nickel from lithium. The precipitate can be calcined to a mixed metal oxide product.

Supplementary Materials: The following supporting information can be downloaded at https://www.mdpi.com/article/10.3390/met12040607/s1, Figure S1: XRD pattern of the leach residue and the reference pattern of manganese citrate monohydrate, $Mn(HC_6H_5O_7)H_2O$ [31]; Figure S2: XRD pattern of the precipitate from the manganese citric acid ethanol system (M7); Figure S3: XRD pattern of the precipitate from the cobalt citric acid ethanol system (C7); Figure S4: XRD pattern of the precipitate from the nickel citric acid acetone system (N8); Figure S5: XRD pattern of the mixed solid phase from the NMC leach liquor acetone system (LNMC4).

Author Contributions: Conceptualization, K.F., A.C. and W.X.; investigation, W.X. and X.X.; formal analysis, W.X., X.X. and R.T.O.; writing—original draft preparation, W.X.; writing—review and editing, all; funding acquisition, A.C. and K.F. All authors have read and agreed to the published version of the manuscript.

Funding: This work was supported by LUE Graduate of Lorraine Université d'Excellence, the French National Research Agency through the national program "Appel à Projet Générique 2018" (ANR-18-CE08-0005-03) and the national program "Investissements d'avenir" with the reference ANR-10-LABX-21- RESSOURCES21. The authors also acknowledge funding from the Swedish Energy Agency (grant numbers 48228-1 and 50122-1).

Data Availability Statement: Not applicable.

Acknowledgments: The authors are grateful to Victor Waller for the exploratory precipitation experiments and literature review, Yiqian Ma for the literature review, Edward Michael Peters and Meher Geetika Sanku for ICP analyses and support in laboratory work, and Chunyan Ma for the fruitful discussions.

Conflicts of Interest: The authors declare no conflict of interest.

References

1. Melin, H.E.; Rajaeifar, M.A.; Ku, A.Y.; Kendall, A.; Harper, G.; Heidrich, O. Global implications of the EU battery regulation. *Science* **2021**, *373*, 384–387. [CrossRef] [PubMed]
2. Armand, M.; Tarascon, J.-M. Building better batteries. *Nature* **2008**, *451*, 652–657. [CrossRef] [PubMed]
3. Boyden, A.; Soo, V.K.; Doolan, M. The Environmental Impacts of Recycling Portable Lithium-Ion Batteries. *Procedia CIRP* **2016**, *48*, 188–193. [CrossRef]
4. Kim, T.; Song, W.; Son, D.-Y.; Ono, L.K.; Qi, Y. Lithium-ion batteries: Outlook on present, future, and hybridized technologies. *J. Mater. Chem. A* **2019**, *7*, 2942–2964. [CrossRef]
5. Chagnes, A.; Swiatowska, J. *Lithium Process Chemistry: Resources, Extraction, Batteries, and Recycling*; Elsevier Science: San Diego, CA, USA, 2015; ISBN 978-0-12-801417-2.
6. Neumann, J.; Petranikova, M.; Meeus, M.; Gamarra, J.D.; Younesi, R.; Winter, M.; Nowak, S. Recycling of Lithium-Ion Batteries—Current State of the Art, Circular Economy, and Next Generation Recycling. *Adv. Energy Mater.* 2022, *in press*. [CrossRef]
7. Moldoveanu, G.A.; Demopoulos, G.P. Organic solvent-assisted crystallization of inorganic salts from acidic media. *J. Chem. Technol. Biotechnol.* **2015**, *90*, 686–692. [CrossRef]
8. Weingaertner, D.A.; Lynn, S.; Hanson, D.N. Extractive crystallization of salts from concentrated aqueous solution. *Ind. Eng. Chem. Res.* **1991**, *30*, 490–501. [CrossRef]
9. Ma, Y.; Svärd, M.; Xiao, X.; Gardner, J.M.; Olsson, R.; Forsberg, K. Precipitation and crystallization used in the production of metal salts for Li-ion battery materials: A review. *Metals* **2020**, *10*, 1609. [CrossRef]
10. Korkmaz, K.; Alemrajabi, M.; Rasmuson, Å.C.; Forsberg, K.M. Separation of valuable elements from NiMH battery leach liquor via antisolvent precipitation. *Sep. Purif. Technol.* **2020**, *234*, 115812. [CrossRef]

11. Cruz, P.; Alvarez, C.; Rocha, F.; Ferreira, A. Tailoring the crystal size distribution of an active pharmaceutical ingredient by continuous antisolvent crystallization in a planar oscillatory flow crystallizer. *Chem. Eng. Res. Des.* **2021**, *175*, 115–123. [CrossRef]
12. Di Profio, G.; Stabile, C.; Caridi, A.; Curcio, E.; Drioli, E. Antisolvent membrane crystallization of pharmaceutical compounds. *J. Pharm. Sci.* **2009**, *98*, 4902–4913. [CrossRef] [PubMed]
13. Diab, S.; Gerogiorgis, D.I. Process modelling, simulation and technoeconomic evaluation of crystallisation antisolvents for the continuous pharmaceutical manufacturing of rufinamide. *Comput. Chem. Eng.* **2018**, *111*, 102–114. [CrossRef]
14. Su, Z.; He, J.; Zhou, P.; Huang, L.; Zhou, J. A high-throughput system combining microfluidic hydrogel droplets with deep learning for screening the antisolvent-crystallization conditions of active pharmaceutical ingredients. *Lab A Chip* **2020**, *20*, 1907–1916. [CrossRef] [PubMed]
15. Zhou, G.X.; Fujiwara, M.; Woo, X.Y.; Rusli, E.; Tung, H.-H.; Starbuck, C.; Davidson, O.; Ge, Z.; Braatz, R.D. Direct Design of Pharmaceutical Antisolvent Crystallization through Concentration Control. *Cryst. Growth Des.* **2006**, *6*, 892–898. [CrossRef]
16. Xuan, W.; de Souza Braga, A.; Chagnes, A. Development of a Novel Solvent Extraction Process to Recover Cobalt, Nickel, Manganese, and Lithium from Cathodic Materials of Spent Lithium-Ion Batteries. *ACS Sustain. Chem. Eng.* **2022**, *10*, 582–593. [CrossRef]
17. Chagnes, A.; Pospiech, B. A brief review on hydrometallurgical technologies for recycling spent lithium-ion batteries: Technologies for recycling spent lithium-ion batteries. *J. Chem. Technol. Biotechnol.* **2013**, *88*, 1191–1199. [CrossRef]
18. Xuan, W.; Otsuki, A.; Chagnes, A. Investigation of the leaching mechanism of NMC 811 ($LiNi_{0.8}$ $Mn_{0.1}$ $Co_{0.1}$ O_2) by hydrochloric acid for recycling lithium ion battery cathodes. *RSC Adv.* **2019**, *9*, 38612–38618. [CrossRef]
19. Xuan, W.; de Souza Braga, A.; Korbel, C.; Chagnes, A. New insights in the leaching kinetics of cathodic materials in acidic chloride media for lithium-ion battery recycling. *Hydrometallurgy* **2021**, *204*, 105705. [CrossRef]
20. Aktas, S.; Fray, D.J.; Burheim, O.; Fenstad, J.; Açma, E. Recovery of metallic values from spent Li ion secondary batteries. *Miner. Process. Extr. Metall.* **2006**, *115*, 95–100. [CrossRef]
21. Meshram, P.; Pandey, B.D.; Mankhand, T.R. Hydrometallurgical processing of spent lithium ion batteries (LIBs) in the presence of a reducing agent with emphasis on kinetics of leaching. *Chem. Eng. J.* **2015**, *281*, 418–427. [CrossRef]
22. Pant, D.; Dolker, T. Green and facile method for the recovery of spent Lithium Nickel Manganese Cobalt Oxide (NMC) based Lithium ion batteries. *Waste Manag.* **2017**, *60*, 689–695. [CrossRef]
23. Xiao, X.; Hoogendoorn, B.W.; Ma, Y.; Ashoka Sahadevan, S.; Gardner, J.M.; Forsberg, K.; Olsson, R.T. Ultrasound-assisted extraction of metals from Lithium-ion batteries using natural organic acids. *Green Chem.* **2021**, *23*, 8519–8532. [CrossRef]
24. Punt, T.; Akdogan, G.; Bradshaw, S.; van Wyk, P. Development of a novel solvent extraction process using citric acid for lithium-ion battery recycling. *Miner. Eng.* **2021**, *173*, 107204. [CrossRef]
25. Okonkwo, E.G.; Wheatley, G.; He, Y. The role of organic compounds in the recovery of valuable metals from primary and secondary sources: A mini-review. *Resour. Conserv. Recycl.* **2021**, *174*, 105813. [CrossRef]
26. Horeh, N.B.; Mousavi, S.M.; Shojaosadati, S.A. Bioleaching of valuable metals from spent lithium-ion mobile phone batteries using Aspergillus niger. *J. Power Sources* **2016**, *320*, 257–266. [CrossRef]
27. Or, T.; Gourley, S.W.D.; Kaliyappan, K.; Yu, A.; Chen, Z. Recycling of mixed cathode lithium-ion batteries for electric vehicles: Current status and future outlook. *Carbon Energy* **2020**, *2*, 6–43. [CrossRef]
28. Gao, W.; Liu, C.; Cao, H.; Zheng, X.; Lin, X.; Wang, H.; Zhang, Y.; Sun, Z. Comprehensive evaluation on effective leaching of critical metals from spent lithium-ion batteries. *Waste Manag.* **2018**, *75*, 477–485. [CrossRef]
29. Golmohammadzadeh, R.; Faraji, F.; Rashchi, F. Recovery of lithium and cobalt from spent lithium ion batteries (LIBs) using organic acids as leaching reagents: A review. *Resour. Conserv. Recycl.* **2018**, *136*, 418–435. [CrossRef]
30. Li, L.; Zhai, L.; Zhang, X.; Lu, J.; Chen, R.; Wu, F.; Amine, K. Recovery of valuable metals from spent lithium-ion batteries by ultrasonic-assisted leaching process. *J. Power Sources* **2014**, *262*, 380–385. [CrossRef]
31. Deng, Y.-F.; Zhou, Z.-H.; Wan, H.-L.; Ng, S.W. **Δ**-Aqua-S-citrato(2–) manganese(II). *Acta Crystallographica. Sect. E Struct.* **2003**, *59*, m310–m312. [CrossRef]
32. Oustadakis, P.; Agatzini-Leonardou, S.; Tsakiridis, P.E. Nickel and cobalt precipitation from sulphate leach liquor using MgO pulp as neutralizing agent. *Miner. Eng.* **2006**, *19*, 1204–1211. [CrossRef]
33. Mohsen-Nia, M.; Amiri, H.; Jazi, B. Dielectric Constants of Water, Methanol, Ethanol, Butanol and Acetone: Measurement and Computational Study. *J. Solut. Chem.* **2010**, *39*, 701–708. [CrossRef]
34. Doki, N.; Kubota, N.; Yokota, M.; Kimura, S.; Sasaki, S. Production of Sodium Chloride Crystals of Uni-Modal Size Distribution by Batch Dilution Crystallization. *J. Chem. Eng. Jpn.* **2002**, *35*, 1099–1104. [CrossRef]
35. Nefedova, K.V.; Zhuravlev, V.D.; Khaliullin, S.M.; Tyutyunnik, A.P.; Buldakova, L.Y. Study of the Composition of a Precipitate Formed from Solutions for the Synthesis of Cathodic Materials Containing Manganese and Citric Acid. *Theor. Found. Chem. Eng.* **2021**, *55*, 117–122. [CrossRef]
36. Lackner, M. *Combustion Synthesis: Novel Routes to Novel Materials*; Bentham Science Publication: Vienna, Austria, 2010; pp. 55–71. ISBN 978-1-60805-155-7.
37. Bohlender, C.; Kahnes, M.; Müller, R.; Töpfer, J. Phase formation, magnetic properties, and phase stability in reducing atmosphere of M-type strontium hexaferrite nanoparticles synthesized via a modified citrate process. *J. Mater. Sci.* **2019**, *54*, 1136–1146. [CrossRef]

38. Demirel, H.S.; Svärd, M.; Uysal, D.; Doğan, Ö.M.; Uysal, B.Z.; Forsberg, K. Antisolvent crystallization of battery grade nickel sulphate hydrate in the processing of lateritic ores. *Sep. Purif. Technol.* **2022**, *286*, 120473. [CrossRef]
39. Matzapetakis, M.; Raptopoulou, C.P.; Tsohos, A.; Papaefthymiou, V.; Moon, N.; Salifoglou, A. Synthesis, Spectroscopic and Structural Characterization of the First Mononuclear, Water Soluble Iron−Citrate Complex, $(NH_4)5Fe(C_6H_4O_7)2{\cdot}2H_2O$. *J. Am. Chem. Soc.* **1998**, *120*, 13266–13267. [CrossRef]
40. Dou, S.; Wang, W. Synthesis and electrochemical properties of layered $LiNi_{0.5} - x\ Mn_{0.5} - x\ Co_{2x}\ O_2$ for lithium-ion battery from nickel manganese cobalt oxide precursor. *J. Solid State Electrochem.* **2011**, *15*, 399–404. [CrossRef]